



Surface Roughness in Abrasive Mixed Rotary Electrical Discharge Machining: Experimental Approach

A. Lamba^{*a}, Vipin^b

^a Department of Mechanical and Automation Engineering, G. B. Pant Okhla-I Campus, DSEU, Delhi, India

^b Department of Mechanical Engineering, Delhi Technological University, Delhi, India

PAPER INFO

Paper history:

Received 22 January 2022

Received in revised form 19 March 2022

Accepted 30 March 2022

Keywords:

Electrical Discharge Machining

D3 Steel

Full Factorial Experimentation

Surface Roughness

Analysis of Variance

ABSTRACT

This research study focused on the alliance of blending silicon carbide powder of size 60 μm into dielectric oil (kerosene) with electrode revolution in electrical discharge machining of D3 steel using electrode made of copper. Peak current, pulse on-time, and electrode revolution were picked as machining variables to check their influence on the surface roughness of the workpiece. The full factorial experimentation was performed with 27 experimental runs. The analysis of variance result indicated electrode revolution as the most influential variable with a percentage aid of 32.75%, followed by peak current and pulse on-time, which accounted for 28.98 and 6.09%, respectively. The decrement in surface roughness was recorded at higher electrode rotational speed. The field emission scanning electron microscopy of machined samples was performed and results showed significant improvement on surface characteristics. The surface finish improved from 12.36 μm to 10.32 μm in silicon carbide powder blended rotational electrical discharge machining over traditional electrical discharge machining. The minimum surface roughness achieved was 4.81 μm at optimal conditions.

doi: 10.5829/ije.2022.35.07a.14

NOMENCLATURE

EDM	Electrical discharge machining	SR	Surface roughness
Pc	Peak current (A)	SiC	Silicon carbide
Pot	Pulse on-time (μs)	ANOVA	Analysis of variance
Erpm	Electrode revolution (rpm)	FESEM	Field emission scanning electron microscopy

1. INTRODUCTION

The ever increasing demand for highly accurate cutting methods has led to the origination of electrical discharge machining (EDM). The material removal in EDM happens with electrical sparks enabling the ejection of tiny debris particles from the workpiece surrounded by EDM fluid. As the sparks generate beneath the electrode's surface, the impression generated on the workpiece's surface replicates the shape of the electrode. The temperature generated by the sparks is of the order of 8000-20000 $^{\circ}\text{C}$ which evaporates the material [1]. The debris thus generated are removed with the help of circulating oil. This cutting style has completely

revolutionized the traditional approach with its extraordinary features like contact-less machining, the ability to cut intricate shapes of material of high hardness including composites with a softer tool material. This method has found a concrete place in almost all machining industries throughout the world. Apart from its many advantages, the process also suffers from disadvantages. The disadvantages include limited material removal capability, difficulty in producing sharp corners in complex shapes, rough surfaces, etc. [2]. In the quest for improvements over these limitations, the researchers initially focused on optimal combinations of input process parameters, and thereafter, as time passed, the focus was shifted to the development of different

*Corresponding author email: ajay.lamba@dseu.ac.in (A. Lamba)

EDM variants. In the past two decades, researchers [3-10] all over the world tailored various successful attempts by their profound search in the domain of electrical discharge machining. These successful attempts by researchers led to the development of different variants resulting in near dry EDM, powder blended EDM, EDM with electrode revolution, vibration-assisted EDM, ultrasonic vibration-assisted EDM, ultrasonic vibration-assisted EDM with a cryogenically cooled electrode, magnetic field-assisted EDM, rotating magnetic field and ultrasonic-assisted EDM, etc. Out of the various research fields, two areas namely, EDM with electrode revolution and powder blended EDM were focused for deeper analysis.

2. LITERATURE SURVEY

The literature review is summarized in Table 1. The presented literature [11-13] showed that surface roughness is improved by electrode revolution [4, 14-17]. It can be seen that the blending of suitable powder type into main dielectric media improved the surface roughness during machining with EDM. In light of these observations [4, 11-17], it was seen that the individual studies are available that improved the same output characteristic i.e. surface roughness. Hence, a research gap was identified by clubbing these two approaches intending to improve the surface roughness even more. Hence, a study involving both electrode revolution and powder blending in the same setup was planned to assess the surface roughness for a work-tool combo of D3 steel

TABLE 1. Summary of literature review

Author	EDM type	W/p material	Tool material	Process parameters	Output responses	Methodology	Findings	Ref.
Chattopadhyay et al.	Rotary EDM	EN8 steel	Cu	peak current, pulse on-time, tool rotation	SR, MRR, EWR	TRD	The study revealed peak current and electrode revolution as highly influential factors affecting SR.	[5]
Shih and Shu	Rotary EDM	AISI D2 tool steel	Cu	discharge depth, electrode rotational speed, discharge direction, polarity, pulse duration, flushing direction, dielectric fluid	SR, MRR, EWR	TRD	1. They claimed minimum surface roughness of 2 μm (R_a) with a negative polarity electrode. 2. Pulse duration and peak current were reported to be the most influential parameters.	[11]
Aliakbari and Baseri	Rotary EDM	X210Cr12 tool steel	Cu	pulse on time, peak current, electrode rotation	SR, MRR, EWR, overcut	TRD	1. They achieved a decreasing trend in the value of SR with the increase in electrode rpm. 2. The minimum surface roughness recorded with a solid electrode, one-eccentric hole electrode, and two-eccentric holes electrode were 5.755 μm , 6.209 μm and 6.68 μm , respectively.	[12]
Dwivedi and Choudhury	Rotary EDM	AISI D3 tool steel	Cu	tool rotation, current	SR	–	1. Electrode revolution caused fewer overall micro-cracks and resulted in a better surface. 2. The improvements in surface characteristics were 10% higher in comparison to stationary EDM i.e. without electrode revolution.	[13]
Kansal et al.	Silicon powder blended EDM	EN31 tool steel	Cu	powder concentration, duty cycle, pulse on-time, peak current	SR, MRR	RSM	1. The apparent improvement in surface characteristics was seen with the use of silicon powder in dielectric oil. 2. SR was mainly affected by peak current and concentration of powder. 3. The lowest SR value was reported at high peak current and powder concentration.	[4]

Bhattacharya et al.	Gr and Al powder blended EDM	EN 31, H 11, HCHCr die steel;	Cu, W-Cu	pulse on-time, pulse off-time, current, powder, electrode, dielectric, w/p material	SR, MRR, TWR	TRD	1. Powder along with other factors such as pulse on-time and peak current significantly affected SR. [14] 2. The surface quality with graphite powder blended oil was found better.
Bhattacharya et al.	Si, Gr, and W powder blended EDM	HCHCr steel, H 11 hot die steel, AISI 1045 steel;	Gr, Br, W-Cu	pulse on-time, current, type of powder, powder concentration	SR, microhardness	TRD	1. The results indicated the improvement in the surface finish of the processed parts. [15] 2. The surface finish was mostly affected by pulse on-time, peak current, and powder concentration.
Singh et al.	Gr powder blended EDM	Super Co 605;	Gr	pulse on-time, pulse off-time, current, polarity, discharge voltage, flushing pressure	microhardness	TRD	The improvement in the surface finish was noted significantly. [16]
Kumar et al.	Alumina powder blended EDM	Inconel 825; copper electrode		pulse on-time, current, gap voltage	SR, MRR, RLT	RSM	1. The average surface roughness obtained with powder blended EDM and conventional EDM was 2.8912 μm and 2.4169 μm , respectively. Furthermore, an average improvement of 0.4743 μm surface roughness was obtained by the proposed PMEDM. [17] 2. At the centre values of parameters (peak current 5A, pulse on-time 7 μs , gap voltage 30V), the improvement claimed was 0.758 μm . 3. The improvement was recorded as a result of a larger inter-electrode gap due to the presence of powder particles, which facilitated better debris removal

Gr – Graphite; Al – Aluminium; HCHCr – High carbon high chromium; Si – Silicon; W – Tungsten; Cu – Copper; W-Cu – Tungsten copper; Br – Brass; RLT – Recast layer thickness; TRD – Taguchi's robust design; RSM – Response surface methodology

and copper. This research work also presents a comparison of surface roughness values obtained with the proposed method to those with conventional EDM for centre values of parameters along with analysis of machined surface through SEM micrographs.

3. MATERIALS AND METHODS

The experiments were performed on a Sparkonix EDM 35A machine. This traditional EDM machine was modified for electrode revolution. For this, a rotary die was fabricated and installed on the EDM head. This rotary die was integrated with the HMC AC servo motor through the chain and sprocket. After this, a separate tank of size (510 mm \times 285 mm \times 160 mm) was also fabricated to add silicon carbide powder of 60-micron particle size with EDM oil (kerosene). The powder concentration was fixed at 6g/l which yielded the finest surface during trial experiments. A small plastic impeller coupled with a stirrer motor shaft was used for continuously stirring the dielectric oil to ensure proper powder circulation in the tank. The stirrer rotational speed in a tank of 17 liters of oil (auxiliary tank) was

measured using a digital tachometer (DT-2234B). The tachometer showed 565 rpm of the shaft. The machining of D3 steel was accomplished using a copper electrode. The size of the workpiece and electrode diameter were (47 mm \times 31 mm \times 7.5 mm) and 20 mm, respectively. Figure 1 illustrates the actual machining setup along with the fabricated rotary die and copper electrode. A comprehensive schematic diagram of the investigational setup is also presented in Figure 2. The elemental constitution of the work material is listed in Table 2. The randomization of run order was performed before conducting the experiments to distribute randomly the variance due to uncontrollable factors. The full factorial experimentation was done by taking three parameters, namely, peak current (Pc), pulse on-time (Pot), and electrode revolution (Erpm) to observe surface roughness as the output characteristic. The pulse-off time value was 30 μs during experiments. The total sparking time was kept fixed at 2 minutes for experimental runs. Table 3 displays the machining variables and their levels. The trials were done in triplicate before the surface roughness measurements were recorded. These values were also evaluated at three different sites on the workpiece's cavity. The average of these readings was noted as a

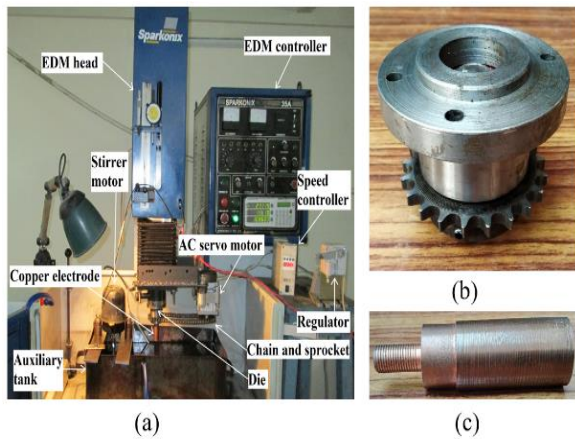


Figure 1. (a) Setup for experimental runs; (b) electrode revolution die; (c) copper electrode

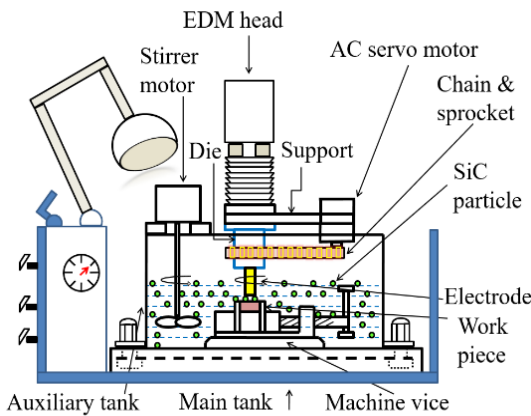


Figure 2. Schematic diagram of the investigational setup

TABLE 2. Elemental constitution of D3 steel

Cr	C	O	Si	Mn	S	P	W	V	Fe
13.40	2.23	2.0	0.41	0.40	0.03	0.05	0.15	0.08	81.25

TABLE 3. Machining variables

Parameter	Unit	Abbreviation	Level		
			1	2	3
Peak current	Ampere (A)	Pc	12	18	24
Pulse on-time	micro-seconds (µs)	Pot	100	400	1000
Electrode revolution	rpm	Erpm	1200	1500	1800

result of each experiment. For measuring SR, Tesa Rugosurf 10G tester was used by fixing a stylus traverse span of 0.8 mm each for 5 cut-offs. The results of surface

roughness are presented in Table 4 along with their input factor level settings.

4. STATISTICAL MODELING OF THE RESPONSE CHARACTERISTIC

To set up a linkage between machining variables and SR of D3 steel, regression analysis of roughness data was done and consequently, a regression equation of 2nd order was developed. Analysis of variance (ANOVA) was done to discover the important terms and interactions between them along with their percentage contributions in surface roughness of D3 steel. The outcomes of ANOVA of SR after removing insignificant terms and interactions will be presented in the next section. Only terms conforming to a P-value (< 0.05) were considered as per 95% confidence interval [18]. During machining, noise due to uncontrollable factors affects the machining results. As a consequence, variation is likely to occur in data. Therefore, an assessment of the range for the predicted model was done encompassing the deviation due to noise. This deviation range [8] was computed by Equation (1). Therefore, prediction by the statistical model can be given by $Y \pm \Delta Y$, where ΔY is given as follows:

$$\Delta Y = t_{\alpha/2,DF} \times \sqrt{V_e} \tag{1}$$

where Y represents response characteristic, t represents the value of t-distribution corresponding to the specified significance level ($\alpha/2 = 0.05$, at 95% confidence interval) and degree of freedom of residual error (DF). V_e represents the residual error of the adjusted mean square. The surface roughness prediction model and the range equation for D3 steel are represented by Equations (2) and (3), respectively.

$$SR = 12.976 + (0.2112 \times Pc) + (0.00489 \times Pot) - (0.006702 \times Erpm) - (0.000011 \times Pot \times Pot) + (0.000004 \times Pot \times Erpm) \tag{2}$$

$$SR_{range} = SR \pm 0.92 \text{ microns} \tag{3}$$

Table 4 summarized 27 experimental runs with machining variables and outcome characteristics.

5. STATISTICAL MODEL VALIDATION

The validation of the statistical model was done by calculating the prediction value supplemented by range with the help of Equations (2) and (3) and thereafter, validating the values thus obtained with experimental results. The results of predicted and experimental findings for arbitrarily chosen run orders 20, 16, 11, and 25 are presented in Table 5. Furthermore, all other values

were also checked and found well within the range. Figure 3 shows the surface roughness versus run order plot for experiment and predicted values. The fitness of the regression predictor can also be ascertained from the distribution of residuals. Figure 4(a-d) depicts the surface roughness residual distribution diagrams illustrating normal probability chart, residual versus fitted value, vertical bar chart, and residual versus observation chart. From Figure 4(a, c), it is evident that all the residuals adhere to a straight line indicating normal distribution. The regression model is thus validated.

TABLE 4. Experimental runs

Run order	Machining variables			Output characteristics			
	Pc (A)	Pot (µs)	Erpm (rpm)	SR			Mean SR (µm)
				1	2	3	
1	12	1000	1500	5.73	6.41	5.59	5.91
2	18	100	1200	10.21	9.6	9.44	9.75
3	18	100	1500	8.86	7.35	7.82	8.01
4	12	100	1500	7.21	7.23	6.83	7.09
5	24	400	1800	9.64	9.89	9.93	9.82
6	12	400	1800	6.13	6.89	6.9	6.64
7	18	100	1800	5.6	6.2	5.42	5.74
8	18	400	1200	10.7	10.31	11.6	10.87
9	18	1000	1800	5.52	5.36	6.07	5.65
10	24	1000	1500	7.71	8.76	8.49	8.32
11	18	400	1500	9.87	11	10.09	10.32
12	24	100	1500	9.3	8.54	8.53	8.79
13	12	1000	1200	6.9	6.97	6.71	6.86
14	12	1000	1800	4.88	5.39	5.36	5.21
15	18	400	1800	7.63	8.71	7.51	7.95
16	12	100	1800	4.83	4.84	4.76	4.81
17	18	1000	1200	7.59	8.26	8.09	7.98
18	24	1000	1200	9.24	8.37	7.86	8.49
19	24	100	1800	6.19	6.7	6.43	6.44
20	12	100	1200	7.6	7.54	8.41	7.85
21	24	400	1500	11.46	10.86	11.04	11.12
22	24	400	1200	12.81	11.79	11.37	11.99
23	24	100	1200	11.36	11.74	11.13	11.41
24	12	400	1500	7.71	7.53	8.43	7.89
25	24	1000	1800	8.7	8.18	7.09	7.99
26	18	1000	1500	6.7	6.84	7.76	7.1
27	12	400	1200	9.11	9.42	9.37	9.3

TABLE 5. Statistical model validation

Run order	Machining variables			SR (microns)	
	Pc (A)	Pot (µs)	Erpm (rpm)	Predicted	Experiment
20	12	100	1200	8.38 ± 0.92	7.85
16	12	100	1800	4.54 ± 0.92	4.81
11	18	400	1500	9.54 ± 0.92	10.32
25	24	1000	1800	7.64 ± 0.92	7.99

6. RESULTS AND DISCUSSION

The effects of peak current (Pc), pulse on-time (Pot), and electrode revolution (Erpm) on SR of D3 steel along with their percentage share are portrayed in Figure 5. This was drawn by taking the mean value of SR at each level of Pc,

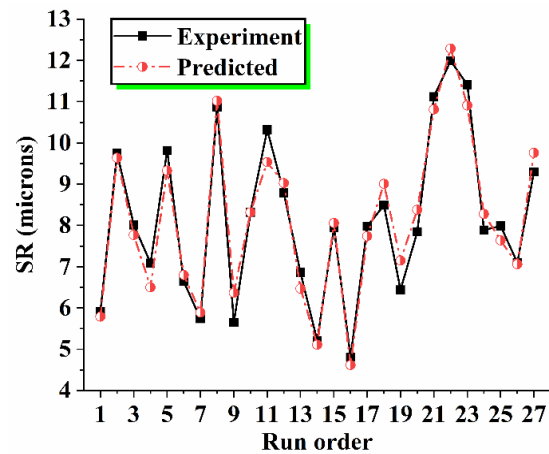


Figure 3. A comparative plot of surface roughness of experiment and predicted values

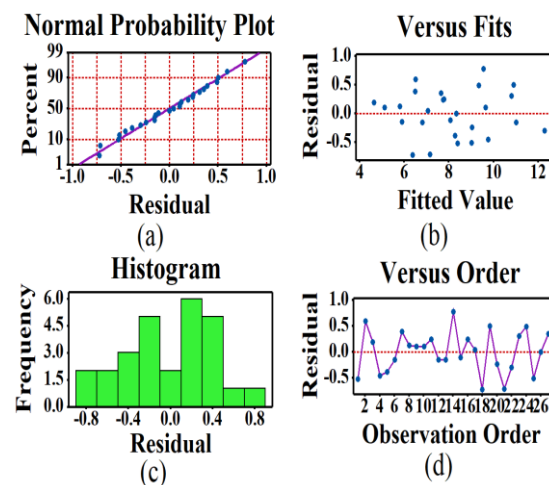


Figure 4. Residual plots of surface roughness (a) normal probability chart; (b) residual versus fitted value; (c) vertical bar chart; (d) residual versus observation order

Pot, and Erpm. Hence, three different mean values are shown for each variable. These mean response values are depicted in Table 6. Furthermore, Figure 6(a-c) depicts the plots of surface roughness versus electrode revolution at different peak currents of 12 A, 18A, and 24 A. From ANOVA outcomes in Table 7, it was found that the highest contribution was made by Erpm followed by Pc and Pot with 32.75, 28.98 and 6.09%, respectively.

6. 1. Effect of Peak Current

Figure 5(a) illustrates the upshot of peak current on SR. It is observed that the rise in peak current results in an increase in SR. The reason may be assigned to the supply of higher energy at a high peak current which leads to deeper craters on the workpiece [19, 20]. These deep craters make the surface rougher, and hence, higher SR was observed [21].

6. 2. Effect of Pulse On-Time

The effect of pulse on-time (Pot) on SR may be witnessed from Figure 5(a). The increase of Pot from 100 μs to 400 μs has been found to increase SR whereas, SR decreased with a further increase in Pot from 400 μs to 1000 μs. The reason may be credited to the widening of the plasma channel at a high Pot. This decreases the spark intensity, ultimately, leading to less energy impact on the work piece, and hence, less crater size [9, 22]. This smoothed the surface for large pulse on-time values such as 1000 μs.

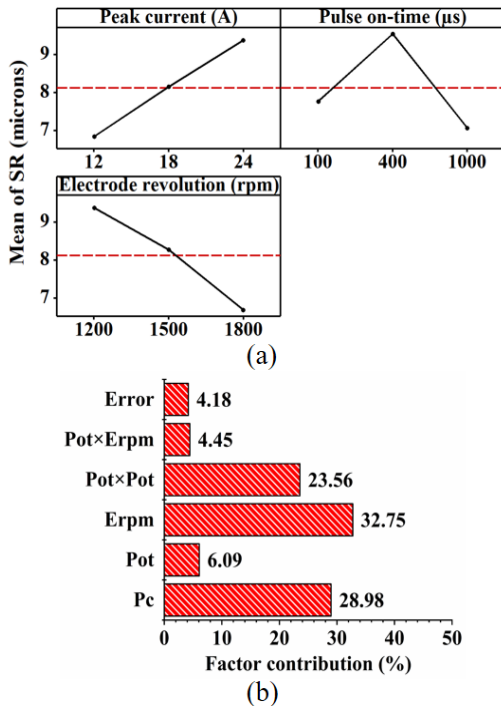


Figure 5. (a) Main effect plot and (b) percentage aid of machining variables on SR

TABLE 6. Response table of means

Level	Pc (A)	Pot (μs)	Erpm (rpm)
1	6.84	7.766	9.389
2	8.152	9.544	8.283
3	9.374	7.057	6.694
Delta	2.534	2.488	2.694
Rank	2	3	1

6. 3. Effect of Electrode Revolution

It may be elucidated from Figure 5(a) and Figure 6(a-c) that the rise in electrode revolution resulted in improvement of rendered surface quality. The rationale of this achievement may be contributed to the efficient cleaning

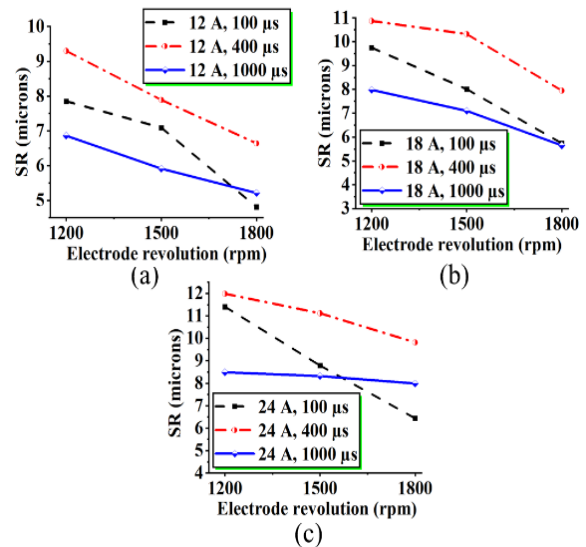


Figure 6. Effect of electrode revolution on surface roughness at peak current (a) 12 A; (b) 18 A; (c) 24 A

TABLE 7. Analysis of variance table for SR

Source	DF	Seq. SS	Share	Adj. SS	Adj. MS	F-Value	P-Value
Regression	5	95.57	95.82%	95.57	19.11	96.29	0.000
Pc	1	28.90	28.98%	28.90	28.90	145.61	0.000
Pot	1	6.07	6.09%	1.39	1.39	7.04	0.015
Erpm	1	32.67	32.75%	26.11	26.11	131.57	0.000
Pot × Pot	1	23.49	23.56%	23.49	23.49	118.36	0.000
Pot × Erpm	1	4.43	4.45%	4.43	4.43	22.34	0.000
Error	21	4.16	4.18%	4.16	0.19		
Total	26	99.74	100.00%				

DF: degree of freedom; Seq. SS: sequential sum of squares; Adj. SS: adjusted sum of squares; Adj. MS: adjusted mean square; F: Fisher's value.

of debris from the machining area. With the increase in electrode revolution, centrifugal force increases, and as the fluid also has abrasive silicon carbide powder, better abrasion, as well as fast cleaning, have benefited the surface, and hence, less surface roughness was obtained [13].

7. INTERACTION EFFECT

Analysis of variance has shown the interaction between pulse on-time and electrode revolution to be inevitable due to a lower P-value than 0.05. Figure 7 depicts the interaction and surface plot of pulse on-time and electrode revolution. The surface roughness of D3 steel was found to increase from 100 to 400 μs and then, decreased from 400 to 1000 μs for all values of electrode revolution. The lower electrode revolution has resulted in a rough surface than the higher rotational values. The minimum surface roughness was recorded at the lowest setting of pulse on-time (100 μs) and the highest setting of electrode revolution (1800 rpm), respectively. The rationale for this particular combination is once again reiterated to the better circulation of dielectric oil facilitated by higher centrifugal force at 1800 rpm of electrode revolution along with abrasive effects of the powder. Simultaneously, the surface finish was augmented by shallow craters due to low-intensity sparks at 100 μs of pulse on-time.

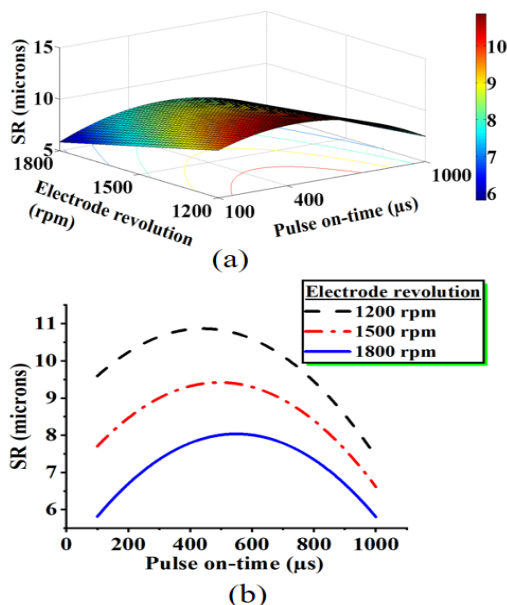


Figure 7. (a) Surface plot; (b) interaction plot of pulse on-time and electrode revolution on SR

8. SURFACE ROUGHNESS PARAMETRIC ANALYSIS

The parametric analysis of surface roughness profiles was executed at Pc-18A, Pot-400 μs and Erpm-1500 rpm with traditional EDM and SiC powder blended rotational EDM. Surface roughness profiles with details of parameters are depicted in Figure 8 for both processes. Three parameters total profile height (Rt), root mean square roughness (Rq), and roughness average (Ra) were measured. The reason for selecting these specific parameters was their capability to explain the entire profile at a glance and acceptance throughout the industries. These parameters in traditional EDM and SiC powder blended rotational EDM were found to be Rt-86.63 μm , Rq-15.85 μm , Ra-12.36 μm , and Rt-70.30 μm , Rq-12.45 μm , Ra-10.32 μm , respectively (refer Figure 8). With these results, the integration of SiC powder blending into EDM oil along with electrode revolution has outperformed the traditional method of EDM machining. The credit of this improvement goes to the efficient dispersal of debris from the inter-electrode gap and formation of shallow craters, facilitated by blending of powder and electrode revolution.

9. SURFACE MORPHOLOGY

Figure 9 shows the result of field emission scanning electron microscopy performed on machined surfaces by traditional EDM and SiC powder blended rotational EDM. The surface images were captured at a magnification of (500 \times) for both the processes and further, images at a magnification of (2000 \times) show the in-depth analysis of crater dimensions. The traditional EDM process resulted in a rough surface and had a lot of cracks and craters (refer Figure 9(a)). An addition of powder and electrode revolution have resulted in a fine surface with fewer cracks (refer Figure 9(b)). Furthermore, the in-depth crater dimension analysis revealed good results with silicon carbide powder blended rotational EDM. The maximum crater depth measured was 18.6 μm in traditional EDM whereas, it was 8.51 μm in SiC powder blended rotational EDM (refer Figure 9(c, d)). These results are a clear reflection of a better surface in SiC powder blended rotational EDM. The reason for the improved surface may be assigned to the efficacious expelling of debris by electrode rotation [13, 23] and higher gap owing to the existence of powder particles blended with EDM oil, which also facilitates effective flushing of debris[17, 24]. Along with this, the intensity of the sparks decreases because of a higher gap between the work piece and electrode leading to the shallow craters, and hence surface finish increases.

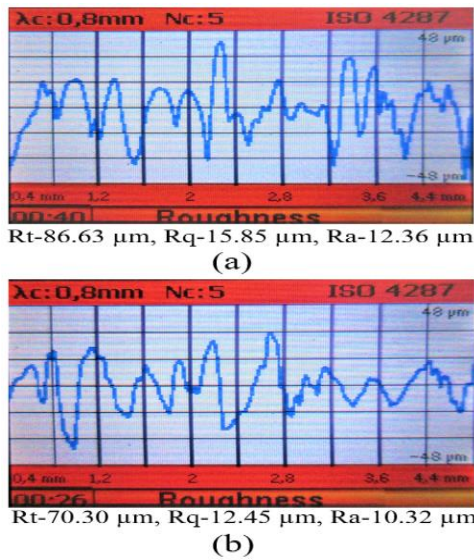


Figure 8. Surface roughness profiles (a) traditional EDM; (b) SiC powder blended rotational EDM. (Pc-18A, Pot-400 μs, Erpm-1500 rpm). (Rt- total profile height, Rq- root mean square roughness, Ra- roughness average)

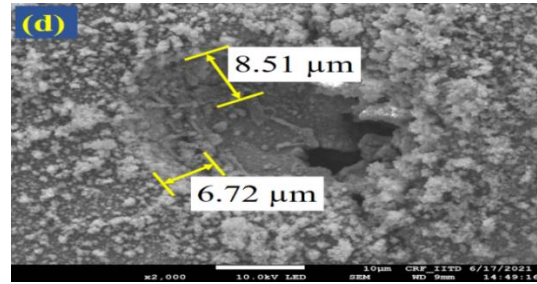
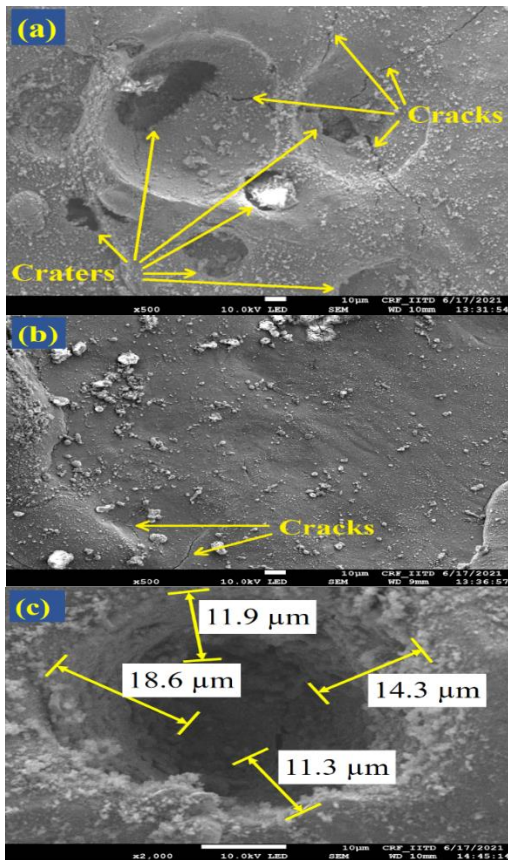


Figure 9. FESEM images of machined samples (a) traditional EDM (500×); (b) SiC powder blended rotational EDM (500×); (c) traditional EDM (2000×) (d) SiC powder blended rotational EDM (2000×). (peak current 18A, pulse on-time 400 μs, electrode revolution 1500 rpm)

10. CONCLUSIONS AND FUTURE SCOPE

The study on surface roughness of D3 steel with the copper electrode in SiC powder blended rotational EDM resulted in the following conclusions:

1. The surface roughness increased with peak current. An increase in SR with pulse on-time was also observed up to 400 μs and a decrease in thereafter.
2. SR reduced with an increase in electrode revolution. An improvement of 28.67% was achieved in the experimented range.
3. The statistical analysis to study the effect of EDM parameters on surface roughness was successfully done.
4. The parametric settings that favoured the highest surface quality were Pc-12A, Pot-100 μs, and Erpm-1800 rpm. At these optimal settings, surface roughness was 4.81 μm.
5. The surface morphology results justified the applicability of SiC powder blended rotational EDM in comparison to the traditional EDM as it led to the creation of fewer cracks and shallow craters on the surface of the work piece. The maximum crater depths were 8.51 μm and 18.6 μm in SiC powder blended rotational EDM and traditional EDM, respectively.
6. The surface roughness profiles recorded with SiC powder blended rotational EDM and traditional EDM have also shown an appreciable decrease in surface roughness (Ra) from 12.36 μm to 10.32 μm.

The future scope of work in the proposed area may be extended with analysis of inter-electrode gap. With exact estimation of gap distance, flushing of debris can be further improved. The spark travel can also be analysed under the influence of electrode rotation as its transverse and inclined travel might affect the discharge crater dimensions.

11. LIMITATIONS

The application of the proposed process is limited to only circular cavity either blind or through-hole as the electrode is under rotation while machining. So, it cannot be used for random cavity/impression generation like for die making.

12. DECLARATION

This research study was conducted without any funding from any agency.

13. REFERENCES

- Ho, K. H., Newman, S. T. "State of the art electrical discharge machining (EDM)", *International Journal of Machine Tools and Manufacture*, Vol. 43, No. 13, (2003), 1287-1300. DOI:10.1016/S0890-6955(03)00162-7
- Qosim, N., Supriadi, S., Puspitasari, P., Kreshanti, P. "Mechanical surface treatments of Ti-6Al-4V Miniplate implant manufactured by electrical discharge machining", *International Journal of Engineering, Transactions A: Basics*, Vol. 31, No. 7, (2018), 1103-1108. DOI:10.5829/ije.2018.31.07a.14
- Puthumana, G., Joshi, S. S. "Investigations into performance of dry EDM using slotted electrodes", *International Journal of Precision Engineering and Manufacturing*, Vol. 12, No. 6, (2011), 957-963. DOI:10.1007/s12541-011-0128-2
- Kansal, H. K., Singh, S., Kumar, P. "Parametric optimization of powder mixed electrical discharge machining by response surface methodology", *Journal of Materials Processing Technology*, Vol. 169, No. 3, (2005), 427-436. DOI:10.1016/j.jmatprotec.2005.03.028
- Chattopadhyay, K. D., Verma, S., Satsangi, P. S., Sharma, P. C. "Development of empirical model for different process parameters during rotary electrical discharge machining of copper-steel (EN-8) system", *Journal of Materials Processing Technology*, Vol. 209, No. 3, (2009), 1454-1465. DOI:10.1016/j.jmatprotec.2008.03.068
- Tong, H., Li, Y., Wang, Y. "Experimental research on vibration assisted EDM of micro-structures with non-circular cross-section", *Journal of Materials Processing Technology*, Vol. 208, No. 1-3, (2008), 289-298. DOI:10.1016/j.jmatprotec.2007.12.126
- Abdullah, A., Shabgard, M. R. "Effect of ultrasonic vibration of tool on electrical discharge machining of cemented tungsten carbide (WC-Co)", *International Journal of Advanced Manufacturing Technology*, Vol. 38, No. 11-12, (2008), 1137-1147. DOI:10.1007/s00170-007-1168-8
- Srivastava, V., Pandey, P. M. "Experimental investigation on electrical discharge machining process with ultrasonic-assisted cryogenically cooled electrode", *Proceedings of the Institution of Mechanical Engineers, Part B: Journal of Engineering Manufacture*, Vol. 227, No. 2, (2013), 301-314. DOI:10.1177/0954405412469487
- Beravala, H., Pandey, P. M. "Experimental investigations to evaluate the effect of magnetic field on the performance of air and argon gas assisted EDM processes", *Journal of Manufacturing Processes*, Vol. 34, (2018), 356-373. DOI:10.1016/j.jmapro.2018.06.026
- Singh, G., Satsangi, P. S., Prajapati, D. R. "Effect of Rotating Magnetic Field and Ultrasonic Vibration on Micro-EDM Process", *Arabian Journal for Science and Engineering*, Vol. 45, No. 2, (2020), 1059-1070. DOI:10.1007/s13369-019-04229-3
- Shih, H. R., Shu, K. M. "A study of electrical discharge grinding using a rotary disk electrode", *International Journal of Advanced Manufacturing Technology*, Vol. 38, No. 1-2, (2008), 59-67. DOI:10.1007/s00170-007-1068-y
- Aliakbari, E., Baseri, H. "Optimization of machining parameters in rotary EDM process by using the Taguchi method", *International Journal of Advanced Manufacturing Technology*, Vol. 62, No. 9-12, (2012), 1041-1053. DOI:10.1007/s00170-011-3862-9
- Dwivedi, A. P., Choudhury, S. K. "Improvement in the Surface Integrity of AISI D3 Tool Steel Using Rotary Tool Electric Discharge Machining Process", *Procedia Technology*, Vol. 23, (2016), 280-287. DOI:10.1016/j.protcy.2016.03.028
- Bhattacharya, A., Batish, A., Singh, G., Singla, V. K. "Optimal parameter settings for rough and finish machining of die steels in powder-mixed EDM", *International Journal of Advanced Manufacturing Technology*, Vol. 61, No. 5-8, (2012), 537-548. DOI:10.1007/s00170-011-3716-5
- Bhattacharya, A., Batish, A., Kumar, N. "Surface characterization and material migration during surface modification of die steels with silicon, graphite and tungsten powder in EDM process", *Journal of Mechanical Science and Technology*, Vol. 27, No. 1, (2013), 133-140. DOI:10.1007/s12206-012-0883-8
- Singh, A. K., Kumar, S., Singh, V. P. "Effect of the addition of conductive powder in dielectric on the surface properties of superalloy Super Co 605 by EDM process", *International Journal of Advanced Manufacturing Technology*, Vol. 77, No. 1-4, (2015), 99-106. DOI:10.1007/s00170-014-6433-z
- Kumar, A., Mandal, A., Dixit, A. R., Das, A. K., Kumar, S., Ranjan, R. "Comparison in the performance of EDM and NPMEDM using Al₂O₃ nanopowder as an impurity in DI water dielectric", *International Journal of Advanced Manufacturing Technology*, Vol. 100, No. 5-8, (2019), 1327-1339. DOI:10.1007/s00170-018-3126-z
- Moghaddam, M. A., Kolahan, F. "Improvement of Surface Finish when EDM AISI 2312 Hot Worked Steel using Taguchi Approach and Genetic Algorithm", *International Journal of Engineering, Transactions C: Aspects*, Vol. 27, No. 3(C), (2014), 417-424. DOI:10.5829/idosi.ije.2014.27.03c.09
- Prakash, K. S., Gopal, P. M., Rahul, R. N. "Effect of material and machining features in electric discharge machining of 6061Al/rock dust composites", *Indian Journal of Engineering and Materials Sciences*, Vol. 27, No. 2, (2020), 471-480
- Singh, S., Maheshwari, S., Pandey, P. C. "Some investigations into the electric discharge machining of hardened tool steel using different electrode materials", *Journal of Materials Processing Technology*, Vol. 149, No. 1-3, (2004), 272-277. DOI:10.1016/j.jmatprotec.2003.11.046
- Phan, N. H., Donga, P. V., Muthuramalingamb, T., Thiena, N. V., Dunga, H. T., Hunga, T. Q., Duca, N. V., Lya, N. T. "Experimental investigation of uncoated electrode and PVD AlCrNi coating on surface roughness in electrical discharge machining of Ti-6Al-4V", *International Journal of Engineering, Transactions A: Basics*, Vol. 34, No. 4, (2021), 928-934. DOI:10.5829/ije.2021.34.04a.19
- Beravala, H., Pandey, P. M. "Experimental investigations to evaluate the surface integrity in the magnetic field and air/gas-assisted EDM", *Journal of the Brazilian Society of Mechanical Sciences and Engineering*, Vol. 43, No. 4, (2021), 213. DOI:10.1007/s40430-021-02929-2
- Bajaj, R., Dixit, A. R., Tiwari, A. K., Chauhan, N. K. "Machining performance enhancement of en-31 die steel using mwcnt mixed rotary edm", *Indian Journal of Engineering and Materials Sciences*, Vol. 27, No. 2, (2020), 309-319.

24. Joshi, A. Y., Joshi, A. Y. "A systematic review on powder mixed electrical discharge machining", *Heliyon*, Vol. 5, No. 12, (2019), e02963. DOI:10.1016/j.heliyon.2019.e02963

Persian Abstract

چکیده

این مطالعه تحقیقاتی بر روی اتحاد پودر کاربید سیلیکون به اندازه ۶۰ میکرومتر به روغن دی الکتریک (نفت سفید) با چرخش الکتروود در ماشینکاری تخلیه الکتریکی فولاد D3 با استفاده از الکتروود ساخته شده از مس متمرکز گردید. جریان پیک، زمان پالس و چرخش الکتروود به عنوان متغیرهای ماشینکاری برای بررسی تأثیر آنها بر زبری سطح قطعه کار انتخاب شدند. آزمایش فاکتوریل کامل با ۲۷ اجرای آزمایشی انجام شد. نتایج تحلیل واریانس نشان داد که چرخش الکتروود به عنوان تأثیرگذارترین متغیر با درصد کمک ۳۲/۷۵ درصد، پس از پیک جریان و پالس به موقع به ترتیب ۲۸/۹۸ و ۶/۰۹ درصد است. کاهش زبری سطح در سرعت چرخش الکتروود بالاتر ثبت گردید. میکروسکوپ الکترونی روبشی گسیل میدانی نمونه های ماشین کاری شده انجام شد و نتایج بهبود قابل توجهی را در ویژگی های سطح نشان داد. پرداخت سطح از ۱۲/۳۶ میکرومتر به ۱۰/۳۲ میکرومتر در ماشینکاری تخلیه الکتریکی چرخشی مخلوط پودر کاربید سیلیکون نسبت به ماشینکاری تخلیه الکتریکی سنتی بهبود یافته است. حداقل زبری سطح به دست آمده ۴/۸۱ میکرومتر در شرایط بهینه بود.
